Effect of Liquid-Solid Contact Angle on Droplet Evaporation

S. Chandra[1], M. di Marzo[2], Y.M. Qiao[1], P. Tartarini[3]

[1] Mechanical Engineering Department
University of Toronto
Toronto, Ontario, Canada M5S 1A4

[2] Mechanical Engineering Department
University of Maryland
College Park, Md, U.S.A. 20742

[3] Istituto di Fisica Tecnica
Universita` di Bologna
viale Risorgimento, 2 - Bologna, Italy 40136

ABSTRACT

The effect of varying initial liquid-solid contact angle on the evaporation of single droplets of water deposited on a stainless steel surface is studied using both experiments and numerical modelling. Contact angle is controlled in experiments by adding varying amounts of a surfactant to water. The evolution of contact angle and liquid-solid contact diameter is measured from a video record of droplet evaporation. The computer model is validated by comparison with experimental results. Reducing contact angle increases contact area between the droplet and solid surface, and also reduces droplet thickness, enhancing heat conduction through the droplet. Both effects increase droplet evaporation rate. Decreasing the initial contact angle from 90° to 20° reduces droplet evaporation time by approximately 50%. The computer model is used to calculate surface temperature and heat flux variation during droplet evaporation: reducing contact angle is shown to enhance surface cooling.

INTRODUCTION

One of the most effective ways of cooling a hot, solid surface is to spray it with liquid droplets. Water sprays are widely used for fire suppression, both to extinguish flames on burning objects and to prevent flame spread by cooling surfaces that have still not ignited. Using excessive amounts of water in fighting fires can, however, cause considerable secondary fire damage, which has motivated research into finding methods to reduce water usage. There is also renewed interest in water as an environmentally benign alternative to halons for fire extinguishment on board aircraft and vehicles, where the weight of liquid that can be carried on board is limited and it is important to minimize water requirements. Efforts to maximize spray cooling efficiencies and optimize water application methods have led to the formulation of models[1-5] to predict heat transfer from a hot surface to an impinging spray. All such simulations incorporate sub-models that describe the evaporation of a single droplet on a hot surface. Several experimental studies have been carried out to observe droplet evaporation[6-13], and both numerical[14,15] and analytical[16-18] models of single droplet evaporation have been developed.

Di Marzo and Evans[14] proposed a model applicable to droplets evaporating on a high thermal conductivity surface at temperatures below those required to initiate nucleate boiling. The analysis was simplified by assuming the solid surface temperature to be constant during droplet evaporation, equal to the contact temperature of two semi-infinite solids. Droplet geometry was described (based on measurements from photographs) by a spherical cap, so that droplet shape was completely specified by the volume of liquid and the liquid-solid contact angle. The reliability of predictions from this model depends both on a correct selection of the initial contact angle and accurate description of its evolution during evaporation. Di Marzo and Evans[14] assumed that the contact angle decreased continuously during droplet evaporation, while the diameter of the wetted region under the droplet remained constant. Observation of water droplets evaporating on an aluminum surface showed this to be a valid assumption over most of the droplet lifetime. However, the assumption of constant liquid-solid contact diameter may not always be accurate. Studies of evaporating droplets[6] have shown that the contact angle cannot decrease beyond a

minimum value, called the receding contact angle[19]. Once this angle has been reached the contact angle remains constant, while the surface area wetted by the droplet decreases. Sadhal and Plesset's model [17] assumes constant contact angle during the entire evaporation process, which is an accurate description of the last stage of droplet evaporation after the receding contact angle is reached. Their results, however, are applicable only to droplets for which the liquid-vapor interface temperature equals that of the ambient vapor.

The contact angle may also be affected by thermal radiation incident upon a droplet. Di Marzo et al.[13] found that infrared radiation is absorbed at the surface of an evaporating droplet, heating it and reducing surface tension. This causes droplets to spread out, increasing liquid-solid contact area and decreasing droplet evaporation time. Such effects may be significant in modelling fire extinguishment by water droplets, and have to be accounted for.

A study of the effect of contact angle on droplet evaporation is important not only in formulating accurate models, but also in suggesting strategies to improve cooling efficiencies by enhancing surface wetting. For example, it is known that the addition of "wetting agents", which are typically surfactant solutions that reduce surface tension, significantly increases the fire extinguishing capabilities of water[20]. Large scale tests have shown that addition of a wetting agent reduces by up to 60% the volume of water required to extinguish fires on wood, cotton bales and rubber tires. Though wetting agents have been used for about 40 years, little information is available on the mechanism by which surfactants enhance heat transfer from a hot surface to impinging droplets in water sprays.

In the present work the effect of varying the initial liquid-solid contact angle on the evaporation of single droplets of water on a hot surface is investigated, using both experiments and numerical modelling. The contact angle is reduced progressively from 90° (the equilibrium value for pure water) to 20°, by adding increasing amounts of surfactant to the liquid. The surface temperature varies from 60°C to 110°C, low enough that nucleate boiling does not occur. In the experiments the initial droplet diameter is held constant (2.05 ± 0.03 mm), as well as surface material (stainless steel), ambient temperature (~20 °C) and ambient pressure (atmospheric). A

stainless steel surface is used since it resists oxidation when heated and can be cleaned easily after deposition and evaporation of droplets, allowing a constant surface condition to be maintained. Stainless steel has a low enough thermal conductivity that the surface cannot be assumed to be isothermal during droplet evaporation: temperature measurements under a droplet evaporating on a low thermal conductivity surface show both spatial and temporal variation[12]. Therefore, the numerical model of di Marzo et al.[15], which couples the solution of the heat conduction equation in both droplet and substrate, is used here to provide a numerical simulation of droplet evaporation.

The main objectives of the present study are: *a*) to investigate experimentally the effect of varying contact angle on the evaporation rate of water droplets; *b*) to measure the evolution of contact angle, contact diameter, and droplet volume during evaporation; *c*) to verify that the numerical model of droplet evaporation accurately predicts the effect of contact angle variation; *d*) to study, using the model, how heat transfer from the solid surface changes with contact angle; and *e*) to examine the possibility of improving spray cooling efficiencies by enhancing surface wetting by droplets.

EXPERIMENTAL METHOD

In the experiments described here, liquid surface tension and liquid-solid contact angle are reduced by dissolving a surfactant, sodium dodecyl sulfate (Malinckrodt Speciality Chemicals), in water. Three surfactant concentrations are used: 0 ppm (i.e., pure water), 100 ppm, and 1000 ppm by weight. Solutions are prepared by adding measured amounts (0.08 g or 0.8 g) of powdered surfactant to 800 g of distilled water. The measured equilibrium contact angle for pure water on a stainless steel surface is 90°; adding 100 ppm and 1000 ppm of surfactant reduces this angle to 55° and 20° respectively. Surfactant concentrations are low enough that other thermophysical properties remain unchanged.

A glass syringe with a plunger driven by a syringe pump is used to form droplets. Water or water/surfactant solution is pumped through stainless steel tubing to a hypodermic needle, at whose tip it accumulate until the weight of liquid exceeds surface tension forces attaching the drop

to the needle. Addition of surfactant reduces the surface tension; the needle diameter is increased to form uniform sized droplets. A 33 gauge needle is used for pure water and 100 ppm solutions, and 30 gauge for 1000 ppm solution droplets. Droplets with diameters of 2.05 mm (pure water), 2.02 mm (100 ppm) and 2.07 mm (1000 ppm) are formed by this method.

Droplets fall from a height of 50 mm onto a stainless steel surface. The droplet impact velocity (1.0 m/s) is low enough that drops remain intact after impact. The stainless steel plate, 50.8 mm square and 6.35 mm thick, is mounted on a copper block in which are housed two 125 W cartridge heaters. The solid surface temperature is measured by a chromel-alumel thermocouple inserted into a hole drilled into the plate. A temperature controller regulates power to the heaters so as to hold the surface temperature prior to droplet deposition constant within $\pm 0.5^\circ$ C.

Measurements of liquid-solid contact angles are sensitive to surface finish and the presence of any contaminants. The stainless steel surface is prepared by polishing with 600 grit emery cloth and metal polish. After the deposition and evaporation of each drop, traces of any residue are removed by cleaning the test surface first with a cotton swab dipped in acetone and then with distilled water. To ensure that surfactant does not accumulate in the syringe, tubing, or needle, the entire system is dismantled before refilling with a solution of different concentration, cleaned by placing it in an acetone bath in an ultrasonic cleaner, dried, and flushed with the new solution. The measured values of the initial contact angle are repeatable within $\pm 3^\circ$.

Droplet evaporation is recorded using a high resolution CCD video camera (Pulnix TM-745). Diffused backlighting is used to illuminate the drop, providing high contrast between the edge of the droplet and its background. Video images of the droplet are imported into a computer-based image analysis package (Image Analyst, Automatix Inc.). Evolution of the droplet-surface contact diameter is measured from the video record, using the image of a 1.6 mm diameter ball bearing to provide a calibration scale. The measurement resolution, corresponding to the size of one video pixel, is ± 0.01 mm. Droplet volume is determined from measurements of the contact diameter and droplet height, assuming the droplet to be a segment of a sphere. Liquid-solid contact angle is measured by using the image analysis software to detect the liquid-air interface in a droplet

image, and approximate it by a straight line. As the image is magnified, this line becomes a tangent to the interface through the liquid-solid-air contact point. The contact angle lies between this tangent and the plane of the solid surface. Values obtained using this automated procedure are checked by manually drawing a tangent through the contact point, and measuring the contact angle. The results obtained by these two methods differ by less than uncertainty in measurement, which is $\pm 2°$.

THEORETICAL MODEL

The model of diMarzo et al.[15] is used here to study the evaporation of a gently deposited droplet on a hot steel surface. It is also used to investigate solid surface temperature and heat flux distribution under droplets, where direct measurements are unavailable. Previous experiments[12] and analyses[15] have shown that the heat flux is neither uniform nor constant during the evaporative process. Most of the evaporation is found to take place at the outer edge of the droplet. Some basic assumptions made in formulating the model are:

- Heat conduction is assumed to be the only heat transfer mechanism in the liquid droplet and in the solid. Nucleate or film boiling are not present.
- The solid surface area wetted by the droplet remains constant when the contact angle is greater than the receding angle.
- After the contact angle reaches the receding angle the aspect ratio of the droplet (assumed to be shaped like a spherical cap) remains constant, while the contact diameter decreases with liquid volume.

Model Formulation

The modeling of the coupled solid and liquid thermal behavior is described by the transient conduction equation for both domains with the appropriate boundary conditions:

$$\text{Solid domain:} \quad \frac{\partial T}{\partial t} = \kappa_s \nabla^2 T \tag{1}$$

$$\text{Liquid domain:} \quad \frac{\partial T}{\partial t} = \kappa_l \nabla^2 T \tag{2}$$

By introducing an overall heat transfer coefficient h at the exposed solid surface, the boundary condition at the liquid-vapor interface can be written as[14]:

$$- k_l \nabla T = h\,(T_i - T_a) + 0.624\, k_c \left(\frac{D}{\kappa_a}\right)^{\frac{2}{3}} \frac{\Lambda}{c_a} \frac{x_i - x_a}{1 - x_a} \tag{3}$$

The boundary conditions at the liquid-solid interface and at the exposed solid surface are:

$$\text{at } 0 \le r \le R, z = 0: \qquad T = T_0;\ k_s \frac{\partial T}{\partial z} = k_l \frac{\partial T}{\partial z} \tag{4}$$

$$\text{at } r > R, z = 0: \qquad k_s \frac{\partial T}{\partial z} = h\,(T_{s0} - T_a) + \varepsilon_s\, \sigma\, (T_s^4 - T_a^4) \tag{5}$$

A linear temperature distribution in the solid is required as initial condition. The far-field temperature distribution is assumed unaffected by droplet evaporation. The liquid droplet is assumed to be initially in thermal equilibrium with the ambient air.

Extremely strong local thermal gradients when the drop initially contacts the surface preclude solution of this problem with conventional finite difference schemes. The solution is obtained by using a Boundary Element Method (BEM) for the solid region and a Control Volume Method (CVM) for the liquid region. The BEM is described in detail by Wrobel & Brebbia[21], while the CVM used here is described by Tartarini et al.[22]. Although the droplet and the solid are treated separately by different numerical methods, the temperatures in the droplet and along the solid surface are solved simultaneously at each time step by coupling the CVM and the BEM in the numerical model. The input variables are: *a*) solid surface material; *b*) solid surface initial temperature; *c*) droplet initial volume; *d*) droplet initial shape factor (β_0); and *e*) the value of the receding contact angle (assumed to be 10° in this study, based on experimental observation). All the physical properties of water and most common solid, non-porous materials have already been implemented into the code. Since droplet shape is assumed to be always that of a spherical cap, liquid-solid contact angle θ is a function of the droplet radius (r) and of the droplet apex (a), that is:

$$\theta = 2\ arctg\left(\frac{a}{r}\right) \tag{6}$$

and it can be calculated at each time step. The validity of this assumption was confirmed by experimental contact angle measurements, shown in the next section.

The model has previously been validated by comparing predictions with experimental data provided by Klassen and di Marzo[9]. A comprehensive comparison of the model with the data is obtained in previous works by looking at the overall predicted evaporation time for aluminum (k = 180 W/m°C) and Macor (k = 1.3 W/m°C) and at the experimental results obtained by Klassen and di Marzo[9], and by di Marzo and Evans[14].

RESULTS AND DISCUSSION

Figure 1 shows photographs of the evaporation of droplets of pure water (0 ppm), and 100 ppm and 1000 ppm surfactant in water solutions on a stainless steel surface initially at a temperature of 80°C. Each column shows successive stages in the evaporation of a droplet; the time of each frame, measured from the instant of impact, is marked. A single bubble is seen in each drop, formed by entrapment of air at the liquid-solid interface during droplet deposition. Increasing surfactant concentration reduces contact angle and increases the liquid-solid contact area. Spreading of the droplet results in a significant decrease in droplet evaporation time: the evaporation time of a 1000 ppm surfactant solution droplet is approximately half that of pure water. Evaporation of a 1000 ppm solution droplet leaves a visible residue of surfactant upon evaporation (figure 1), which is cleaned before deposition of another droplet.

To confirm that the numerical simulation accurately models droplet evaporation, code predictions are compared with experimental results over the entire range of surface temperatures used in experiments. Figure 2 shows both experimental measurements and numerical code predictions of volume evolution during evaporation of pure water droplets at three surface

temperatures: 60°C, 80°C and 100°C. Good agreement is seen between measured and predicted values at all surface temperatures.

The model also accurately predicts the increased evaporation rate of droplets whose initial contact angle is reduced by addition of a surfactant. Figure 3 shows a comparison between measurements and code predictions of volume evolution for droplets with 0, 100 and 1000 ppm surfactant added, on a stainless steel surface at 80°C. Reduction in evaporation time because of adding surfactant is summarized in figure 4, which shows droplet evaporation time for $60°C \leq T_S \leq 110°C$. Solid surface temperature above 110°C cause the onset of nucleate boiling, for which the code is no longer applicable. Evaporation time is reduced to approximately 75% and 50% of that of pure water drops by addition of 100 ppm and 1000 ppm surfactant respectively. This reduction in evaporation time is correctly predicted by the numerical code.

Figure 5 shows the measured variation of contact angle during droplet evaporation. A pure water drop has a large initial contact angle (90°±3°). The contact angle decreases as the droplet evaporates, while contact diameter remains unchanged. Corresponding measurements of the diameter wetted by the same drop are shown in figure 6. The contact diameter remains almost constant until the end of the droplet lifetime, as assumed by di Marzo & Evans [14] in modelling droplet evaporation. Adding 100 ppm of surfactant to a water droplet reduces the initial contact angle to 55°±3° (figure 5). The contact angle decreases until it reaches the value of the receding contact angle, which is measured to be 10° and is not changed by addition of surfactant to water. The contact angle then remains constant, while the contact diameter decreases (figure 6). Droplets with 1000 ppm of surfactant have a low initial contact angle (20°±3°). On evaporation the contact angle rapidly reaches the receding value, and is then constant over most of the droplet lifetime. The computer code provides an accurate description of the variation of both contact angle and contact diameter during droplet evaporation.

Decreased droplet evaporation time when contact angle is reduced by adding a surfactant can have two possible causes. Firstly, droplet contact diameter becomes larger, increasing the area for heat transfer from the solid to liquid. Secondly, when the droplet spreads and the liquid layer

becomes thinner heat transfer to the liquid-vapor interface rises, increasing the interface temperature and the saturation vapor pressure at the droplet surface. If this second effect is significant, we expect to see an increase in heat flux from the solid surface to the droplet when initial contact angle is reduced. Figure 7 shows the calculated variation of local heat flux at the center of the surface area wetted by drops evaporating on a surface initially at 80°C, and it confirms that adding 100 ppm or 1000 ppm of surfactant produces a small increase in heat flux. In all three cases (0 ppm, 100 ppm and 1000 ppm) heat flux increases towards the end of droplet lifetime, as droplets evaporate and become thinner. However, increase in surface area wetted by the drop is the more important effect of contact angle reduction, as seen in figure 8 which plots calculated values of the heat flux averaged over the entire wetted area. Addition of surfactant reduces the average heat flux, indicating that increased local heat flux is offset by the larger area wetted by the drop.

The increased effectiveness of droplets in cooling a hot surface when surfactant is added can be demonstrated through comparing temperature profiles in the substrate during droplet evaporation. In figures 9*a-c* the evolution of temperature is shown in a solid surface initially at 80°C, on which droplets with 0 ppm, 100 ppm or 1000 ppm of dissolved surfactant are deposited. Temperature profiles are shown at 10% (figure 9*a*), 50% (figure 9*b*) and 90% (figure 9*c*) respectively of the total evaporation time of each droplet. Temperatures are plotted against a normalized coordinate obtained by dividing the radial distance from the center of the wetted region by the radius of a spherical droplet (R_{sphere} = 1.0 mm in our experiments). Surface temperature is lowest at the center of each droplet, and increases towards its edge. Addition of a surfactant is seen to both significantly enhance cooling at the droplet center, as well as to increase the radius over which surface temperature is lowered by the droplet.

Both experiments and the numerical model have shown that varying initial liquid-solid contact angle can significantly change droplet evaporation time. Figure 10 summarizes the effect of reducing contact angle on evaporation time of droplets on a stainless steel surface initially at 80°C, showing that reducing the initial contact angle from 90° to 20° (the range in our experiments) decreases the evaporation time by approximately 50%. Models of spray evaporation therefore

require accurate information about the initial contact angle to realistically simulate fire extinguishment. These observations also help explain why adding a wetting agent improves the fire extinguishing capabilities of water.

CONCLUSIONS

The cooling of a hot solid surface by evaporation of a liquid droplet has been studied using both experiments and numerical modelling. The effect of varying liquid-solid contact angle on droplet evaporation has been investigated in detail. The model was validated by comparing predictions of droplet evaporation time with experimental measurements, for a range of surface temperatures ($60°C \leq T_S \leq 110°C$) and initial contact angles ($20° \leq \theta_0 \leq 90°$). Addition of a surfactant to a water droplet reduces surface tension and increases its spreading on a solid surface. As the liquid layer becomes thinner, heat transfer from the solid to the liquid-vapor interface is enhanced. Spreading of the droplet also increases the heat transfer area. Both these effects contribute to a faster evaporation rate: decreasing contact angle from 90° to 20° reduced droplet evaporation time by approximately 50%.

ACKNOWLEDGEMENTS

This study was made possible by a grant of the Building and Fire Research Laboratory, National Institute of Standards and Technology. Funding of the computational expenditures was provided by the Italian M.U.R.S.T. and C.N.R. Experiments were funded by a grant from the Canadian N.S.E.R.C.

NOMENCLATURE

a	droplet apex
c	specific heat
D	air-steam mass diffusivity
h	overall heat transfer coefficient
h_c	convective heat transfer coefficient
k	thermal conductivity
r	radial coordinate
R	radius of the wetted area
t	time
T	temperature
x	molar fraction of steam in air
z	axial coordinate

Greek letters

β	shape parameter
ε	emissivity
θ	solid-liquid contact angle
κ	thermal diffusivity
Λ	liquid latent heat of vaporization
σ	Stefan-Boltzmann constant

Subscripts

a	air
i	interfacial
l	liquid
s	solid sphere
0	initial

REFERENCES

1. Toda, S., A study of mist cooling. First report:investigation of mist cooling. *Heat Transfer - Japanese Research* **1**(3), 39-50 (1972).

2. Bonacina, C., Del Giudice, S. & Comini, G., Dropwise Evaporation. *Transactions of the ASME- Journal of Heat Transfer* **101**, 441-446 (1979).

3. Rizza, J. J., A numerical solution to dropwise evaporation. *Transactions of the ASME, Journal of Heat Transfer* **103**, 501-507 (1981)

4. Bolle, L. & Moreau, J. C., Spray cooling of hot surfaces. *Multiphase Science and Technology* **1**, 1-97 (1982).

5. Tio, K. K. & Sadhal, S. S., Dropwise evaporation: thermal analysis of multidrop systems. *International Journal of Heat and Mass Transfer* **35**, 1987-2004, (1992).

6. Simon, F. F. & Hsu, Y. Y., Wetting dynamics of evaporating drops on various surfaces. NASA TM X-67913 (1971).

7. Michiyoshi, I. & Makino, K., Heat transfer characteristics of evaporation of a liquid droplet on heated surfaces. *International Journal of Heat and Mass Transfer* **21**, 605-613 (1978).

8. Zhang, N. & Yang, W. J., Evaporative convection in minute drops on a plate with temperature gradient. *International Journal of Heat and Mass Transfer* **26**, 1479-1488 (1983).

9. Klassen, M. & di Marzo, M., Transient cooling of a hot surface by droplets evaporation. NIST-GCR-90-575 (1990).

10. Xiong, T. Y. & Yuen, M. C., Evaporation of a liquid droplet on a hot plate. *International Journal of Heat and Mass Transfer* **34**, 1881-1894, (1991).

11. Rymkiewicz, J. & Zapalowicz, Z., Analysis of the evaporation process for water droplet on flat heated surface. *International Communications in Heat and Mass Transfer* **20**, 687-697 (1993).

12. Abu-Zaid, M. & Atreya, A., Transient cooling of hot porous and nonporous ceramic solid by droplet evaporation. *Transactions of the ASME-Journal of Heat Transfer* **116**, 694-701 (1994).

13. di Marzo, M. & Evans, D. D., Evaporation of a water droplet deposited on a hot high thermal conductivity surface. *Transactions of the ASME-Journal of Heat Transfer* **111**, 210-213 (1989).

14. di Marzo, M., Tartarini, P., Liao, Y., Evans, D. & Baum, H., Evaporative cooling due to a gently deposited droplet. *International Journal of Heat and Mass Transfer* **36**, 4133-4139 (1993).

15. di Marzo, M., Kidder, C. H. & Tartarini, P., Infrared thermography of dropwise evaporative cooling of a semi-infinite solid subjected to radiant heat input, *Experimental Heat Transfer* **5**, 101-114 (1992).

16 Yang, W. J., Mechanics of droplet evaporation on heated surfaces. *Letters in Heat and Mass Transfer* **5**, 151-166 (1978).

17. Sadhal, S. S. & Plesset, M. S., Effect of solid properties and contact angle in dropwise condensation and evaporation. *Transactions of the ASME-Journal of Heat Transfer* **101**, 48-54 (1979).

18. Tio, K. K. & Sadhal, S.S., Thermal analysis of droplet spray evaporation from a heated solid surface. *Transactions of the ASME-Journal of Heat Transfer* **114**, 220-233 (1992).

19. Herzberg, W. J. & Marian, J. E., The receding contact angle. *Journal of Colloid and Interface Science* **33**, 164-171 (1970).

20. Bryan, J. L., Fire Suppression and Detection Systems, 3rd edition, Macmillan Publishing Company, New York , 331-334 (1993).

21. Wrobel, L.C. & Brebbia, C.A., A Formulation of the Boundary Element Method for Axisymmetric Transient Heat Transfer Conduction. *International Journal of Heat and Mass Transfer* **24**, pp. 843-850 (1981).

22. Tartarini, P., Liao, Y. & diMarzo, M., Transient Cooling of a Hot Surface by Droplets Evaporation. UMCP Mechanical Engineering Report, No. 90-6 (1990).

FIGURE CAPTIONS

Figure 1 The evaporation of droplets of pure water (0 ppm), 100 ppm and 1000 ppm surfactant solutions on a stainless steel surface at 80°C.

Figure 2 Comparison of code predictions (solid lines) with measured (symbols) volume evolution during evaporation of pure water droplets on a stainless steel surface at 60°C, 80°C and 100°C.

Figure 3 Comparison of code predictions (solid lines) with measured (symbols) volume evolution during evaporation of droplets of pure water (0 ppm), 100 ppm and 1000 ppm surfactant solutions on a stainless steel surface at 80°C.

Figure 4 The evaporation time of droplets of pure water (0 ppm), 100 ppm and 1000 ppm surfactant solutions on a stainless steel surface at initial surface temperatures ranging from 60°C to 110°C.

Figure 5 Evolution of contact angle during evaporation of droplets of pure water (0 ppm), 100 ppm and 1000 ppm surfactant solutions on a stainless steel surface at 80°C.

Figure 6 Evolution of liquid-solid contact diameter during evaporation of droplets of pure water (0 ppm), 100 ppm and 1000 ppm surfactant solutions on a stainless steelsurface at 80°C.

Figure 7 Calculated variation of local heat flux at the center of the surface area wetted by droplets evaporating on a stainless steel surface initially at 80 C.

Figure 8 Calculated values of heat flux averaged over the entire wetted area during droplet evaporation on a surface initially at 80 C.

Figure 9 Calculated temperature profiles in a solid surface initially at 80°C, during evaporation of droplets of pure water (0 ppm), 100 ppm and 1000 ppm surfactant solutions at *a*) 10%, *b*) 50%, and *c*) 90% of the total evaporation time.

Figure 10 Effect of reducing contact angle on evaporation time of droplets on a stainless steel surface initially at 80°C.

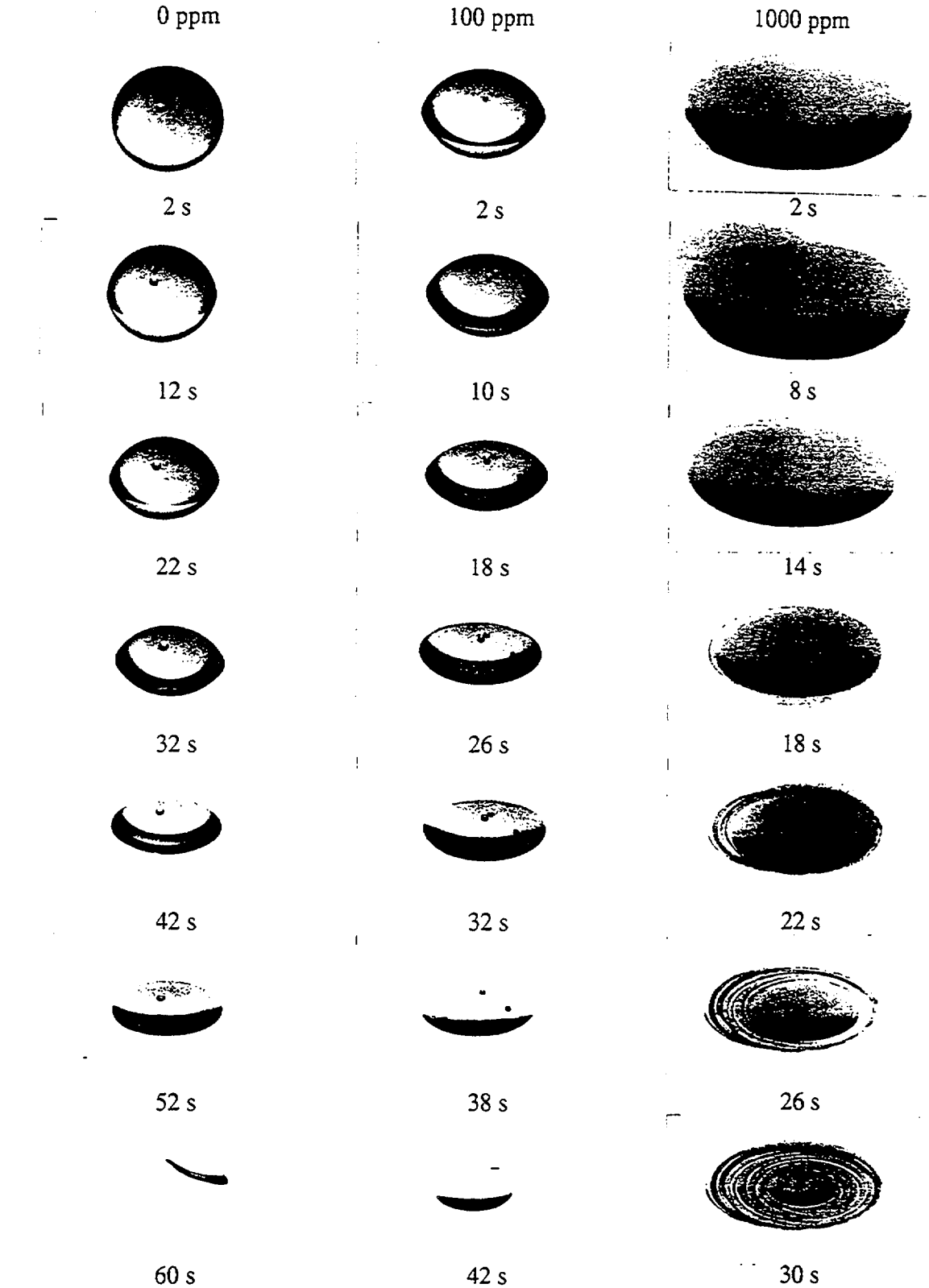

Figure 1 The evaporation of droplets of pure water (0 ppm), 100 ppm and 1000 ppm surfactant solutions on a stainless steel surface at 80°C.

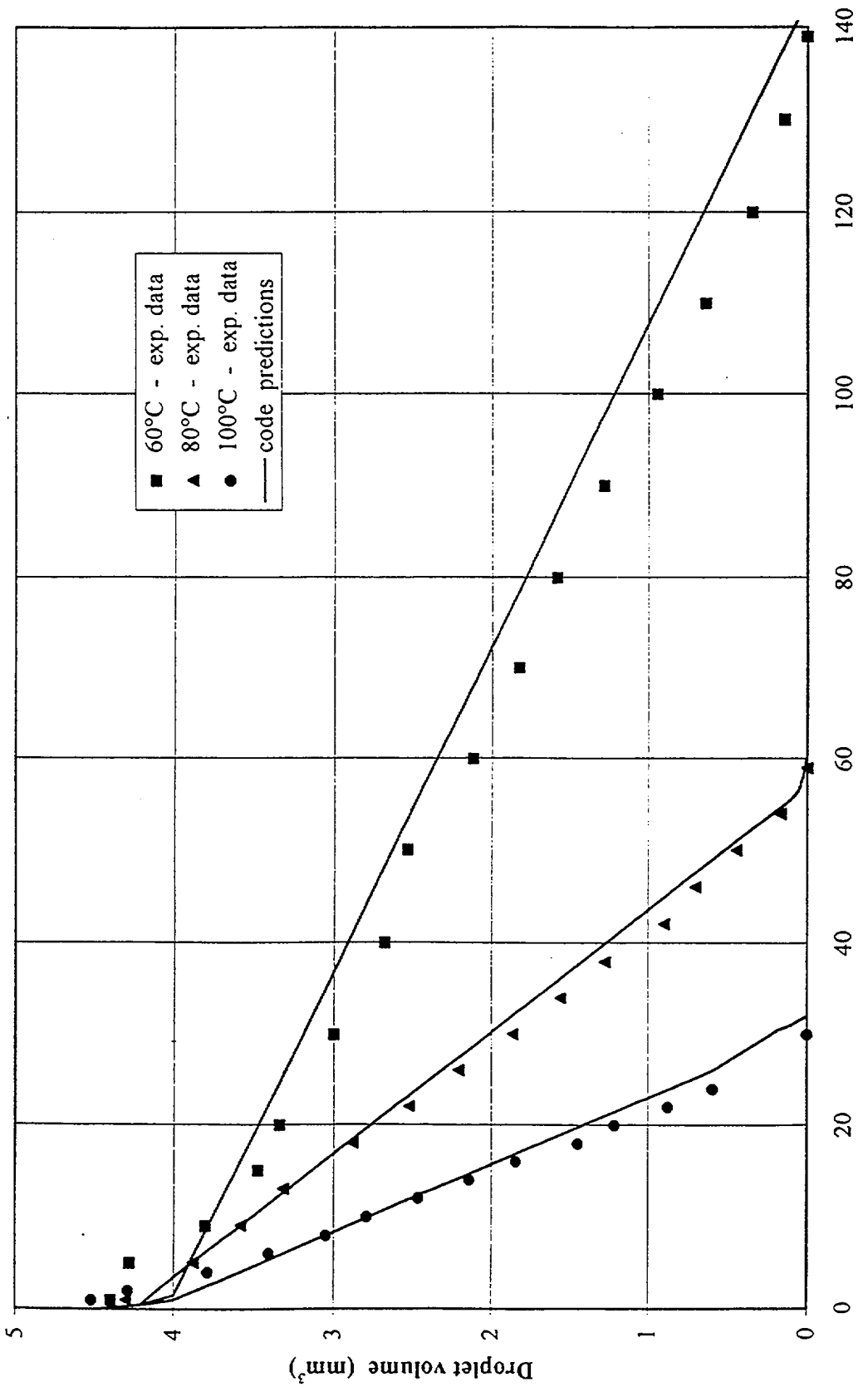

Figure 2 Comparison of code predictions (solid lines) with measured (symbols) volume evolution during evaporation of pure water droplets on a stainless steel surface at 60°C, 80°C and 100°C.

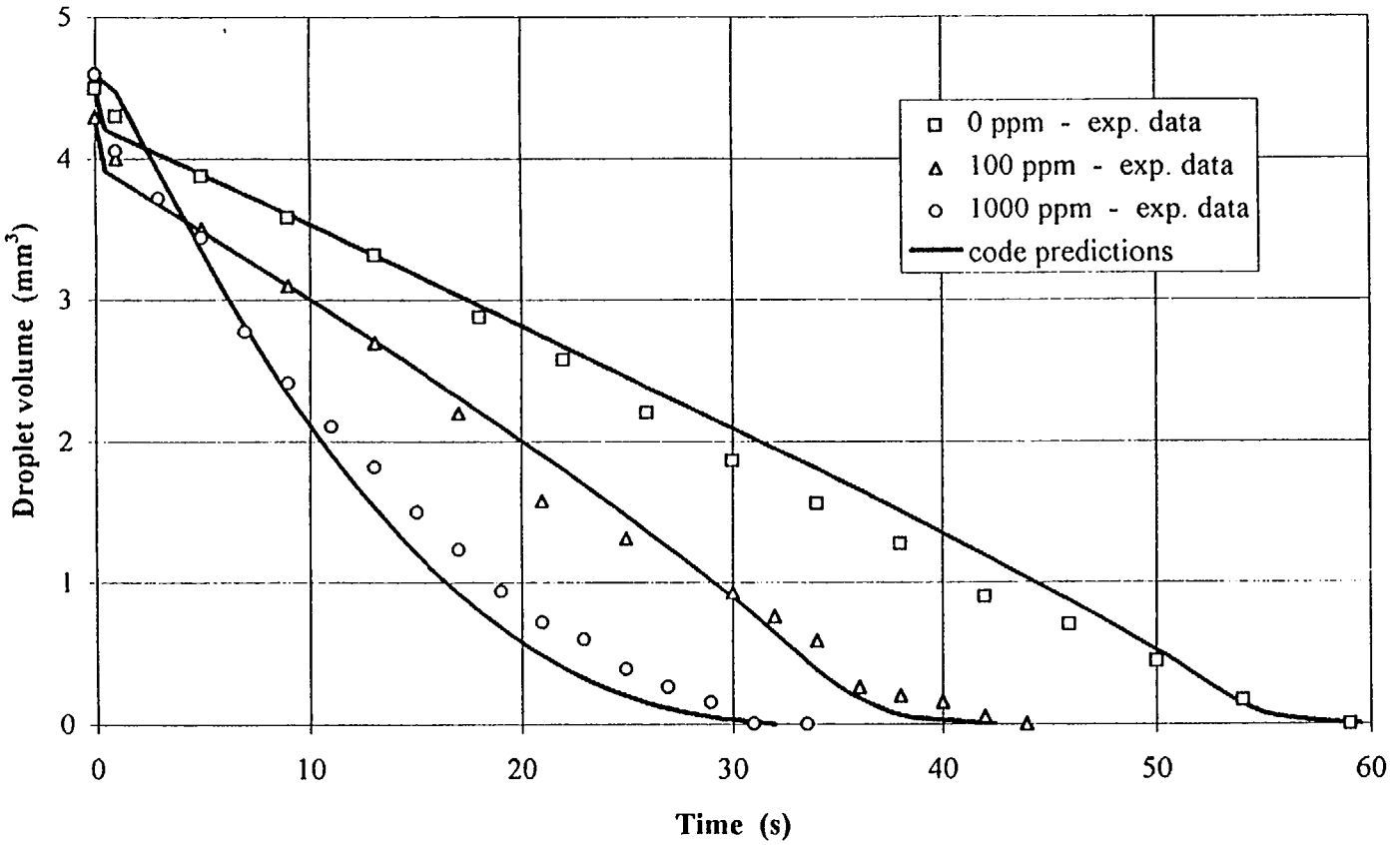

Figure 3 Comparison of code predictions (solid lines) with measured (symbols) volume evolution during evaporation of droplets of pure water (0 ppm), 100 ppm and 1000 ppm surfactant solutions on a stainless steel surface at 80°C.

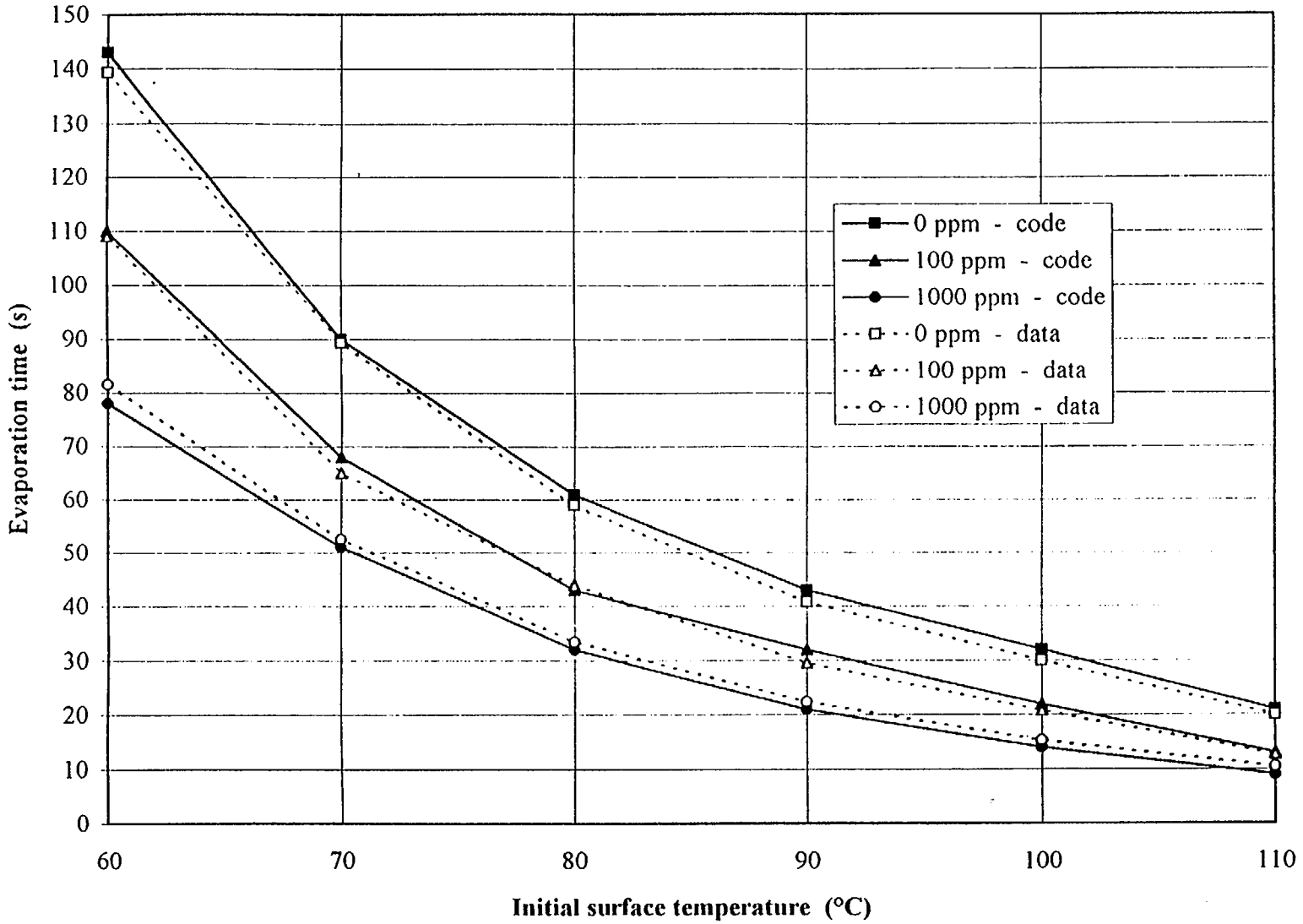

Figure 4 The evaporation time of droplets of pure water (0 ppm), 100 ppm and 1000 ppm surfactant solutions on a stainless steel surface at initial surface temperatures ranging from 60°C to 110°C.

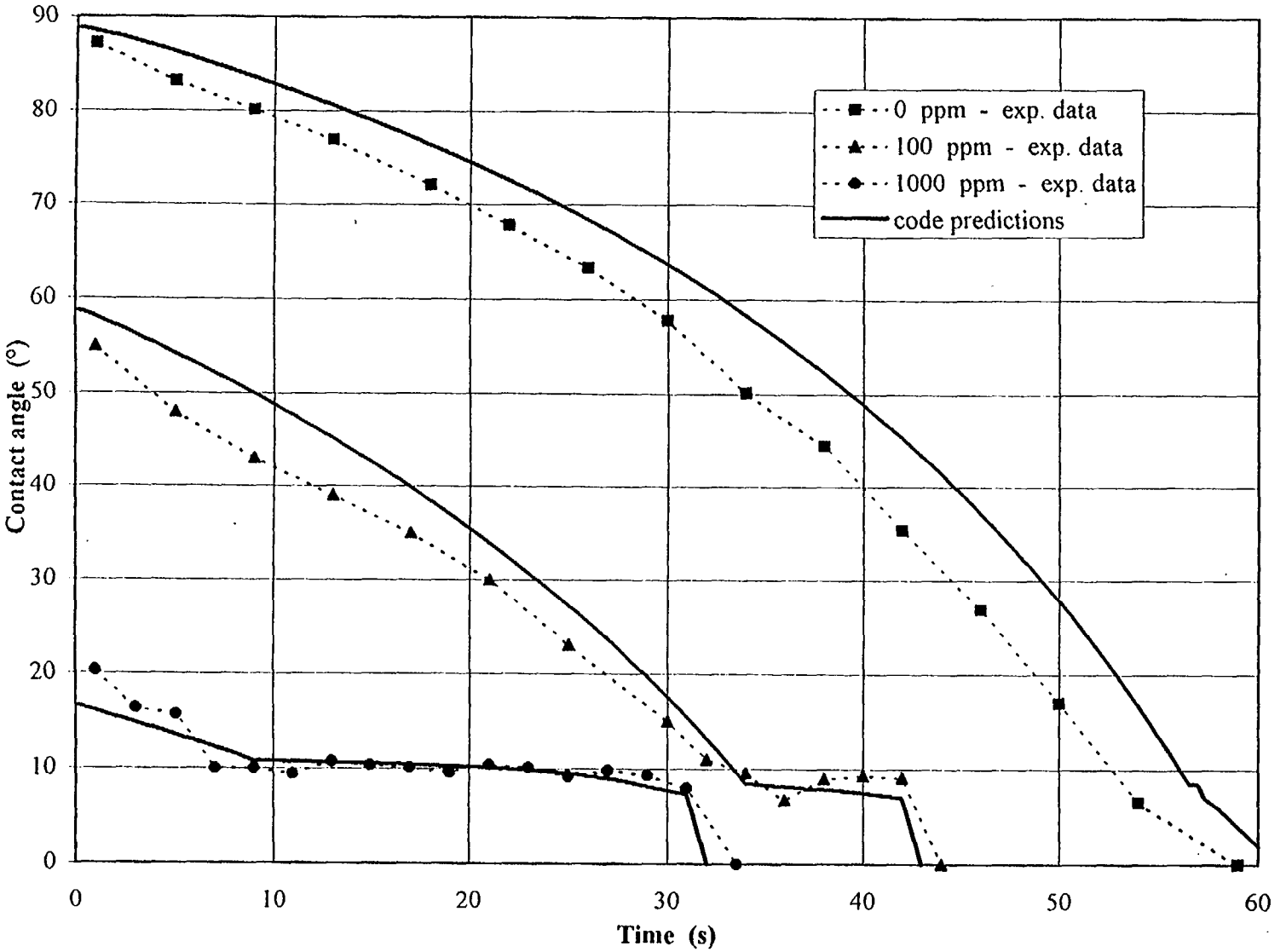

Figure 5 Evolution of contact angle during evaporation of droplets of pure water (0 ppm), 100 ppm and 1000 ppm surfactant solutions on a stainless steel surface at 80°C.

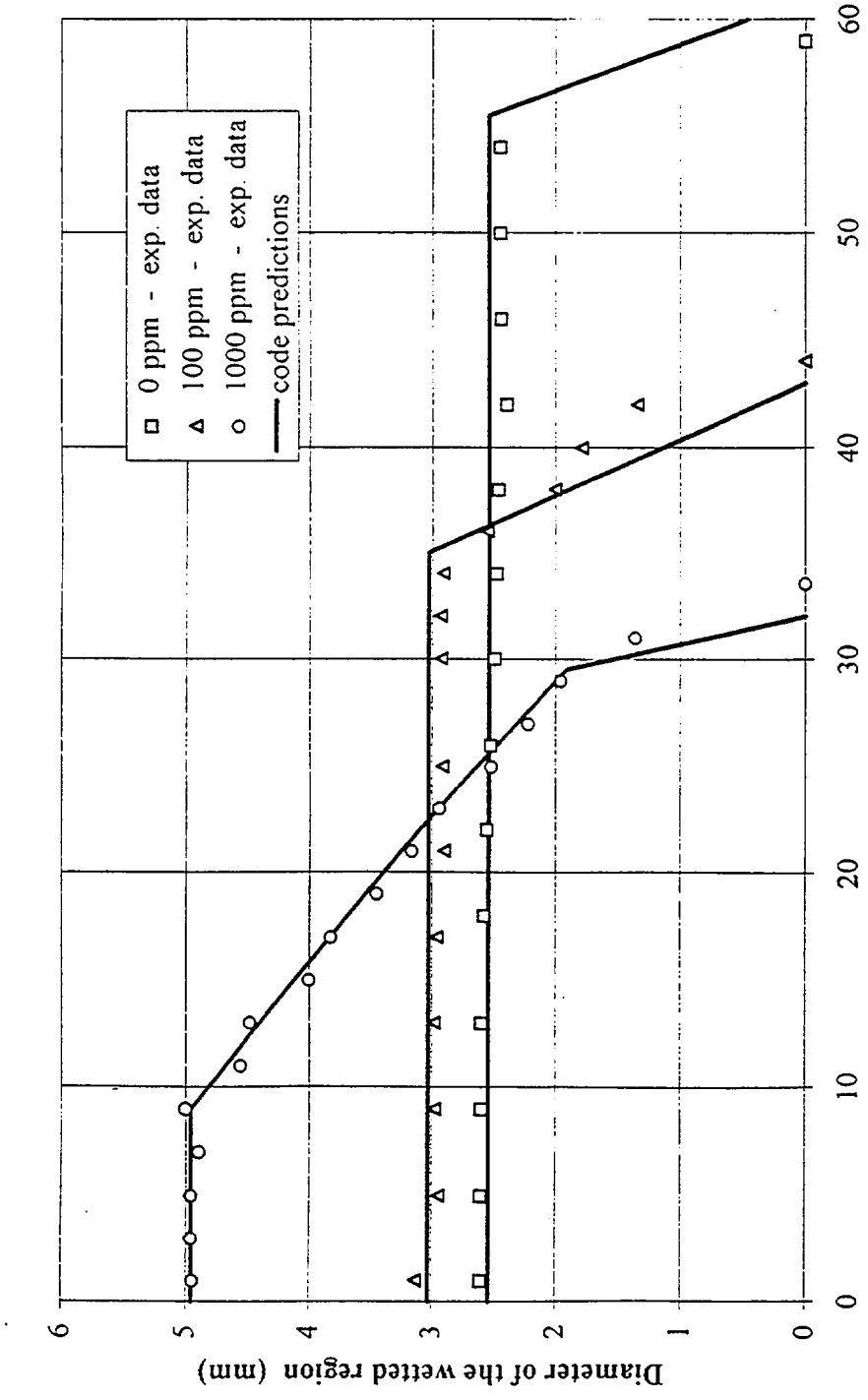

Figure 6 Evolution of liquid-solid contact diameter during evaporation of droplets of pure water (0 ppm), 100 ppm and 1000 ppm surfactant solutions on a stainless steel surface at 80°C.

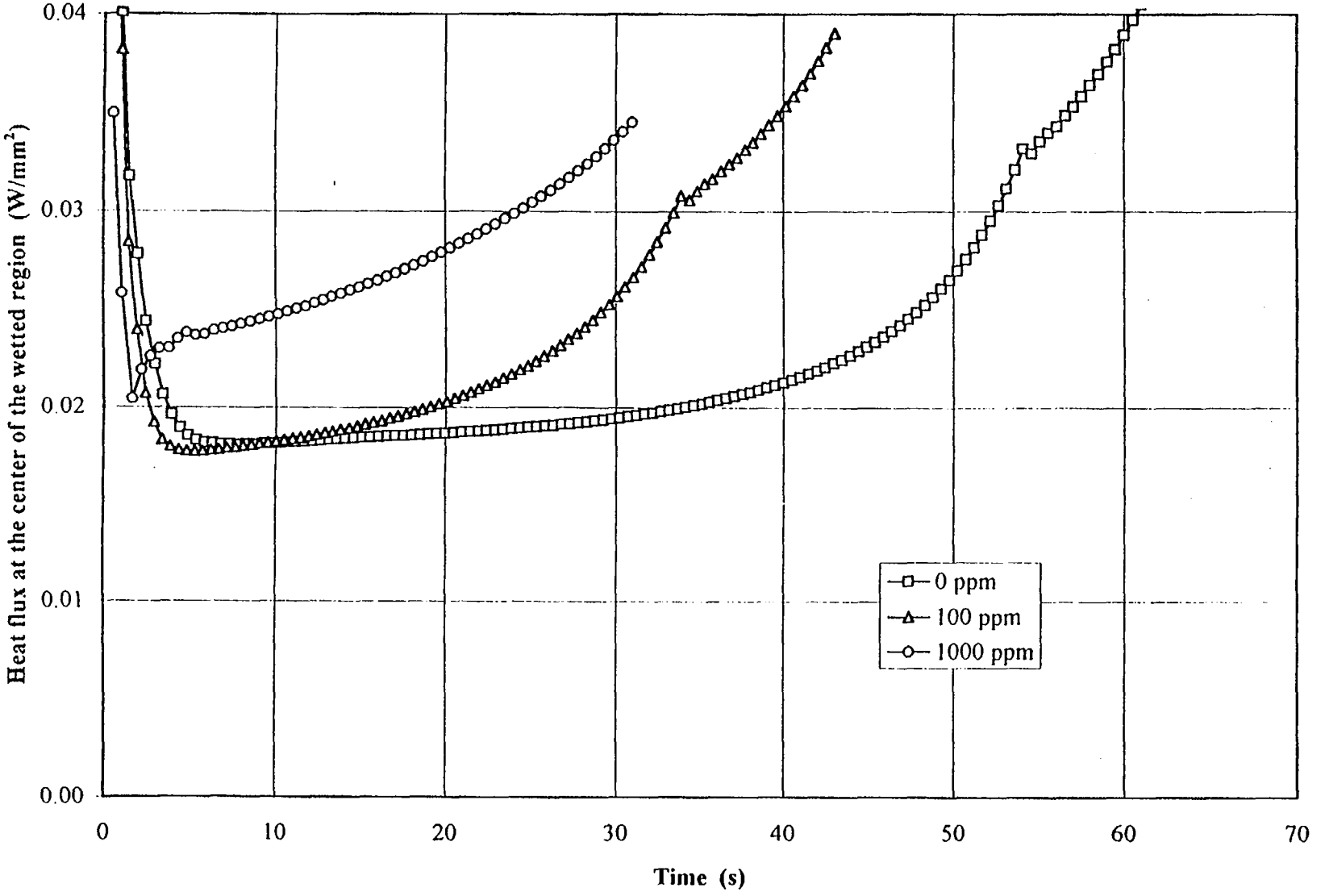

Figure 7 Calculated variation of local heat flux at the center of the surface area wetted by droplets evaporating on a stainless steel surface initially at 80°C.

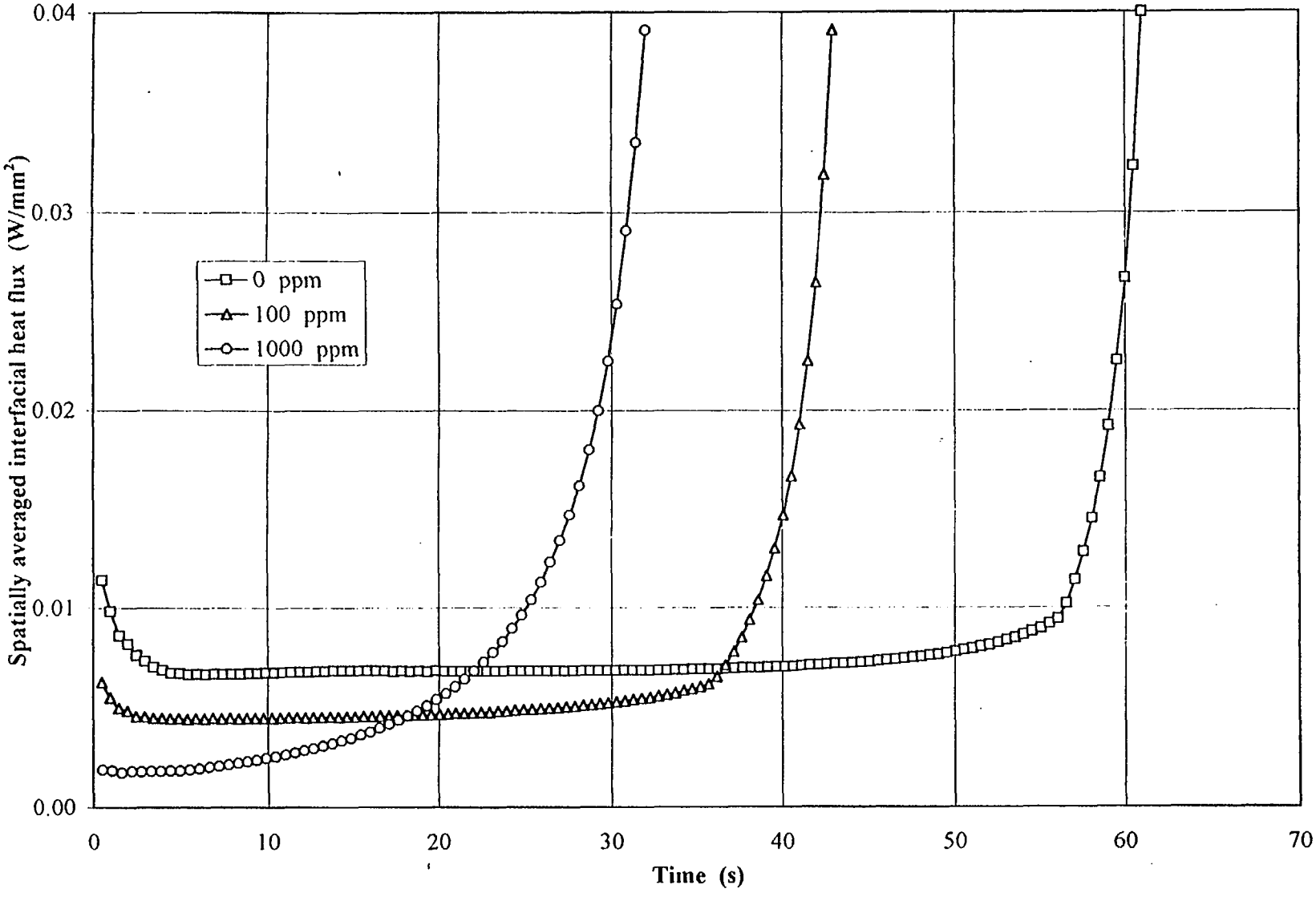

Figure 8 Calculated values of heat flux averaged over the entire wetted area during droplet evaporation on a surface initially at 80°C.

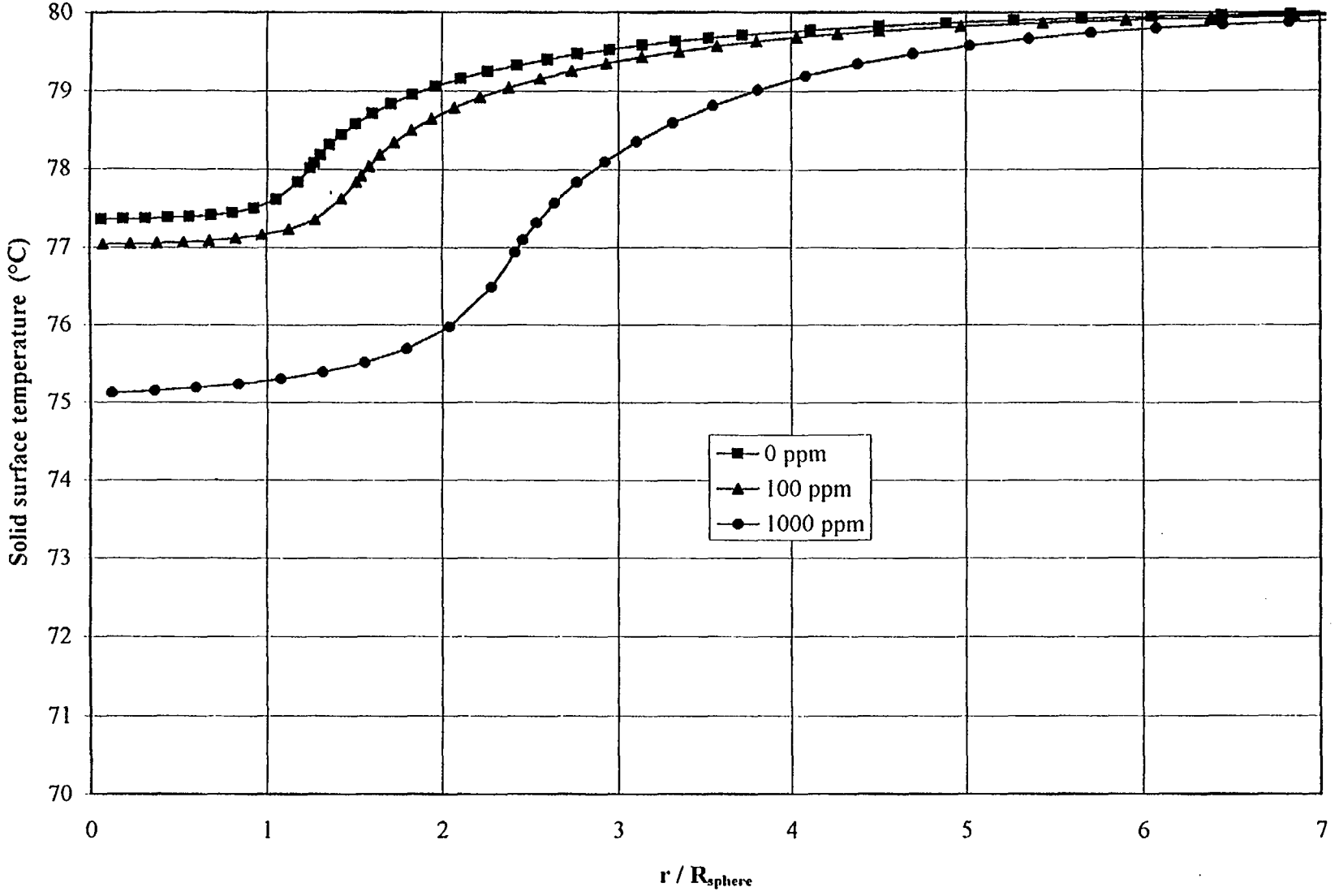

Figure 9 Calculated temperature profiles in a solid surface initially at 80°C, during evaporation of droplets of pure water (0 ppm), 100 ppm and 1000 ppm surfactant solutions at *a*) 10%, *b*).50%, and *c*) 90% of the total evaporation time

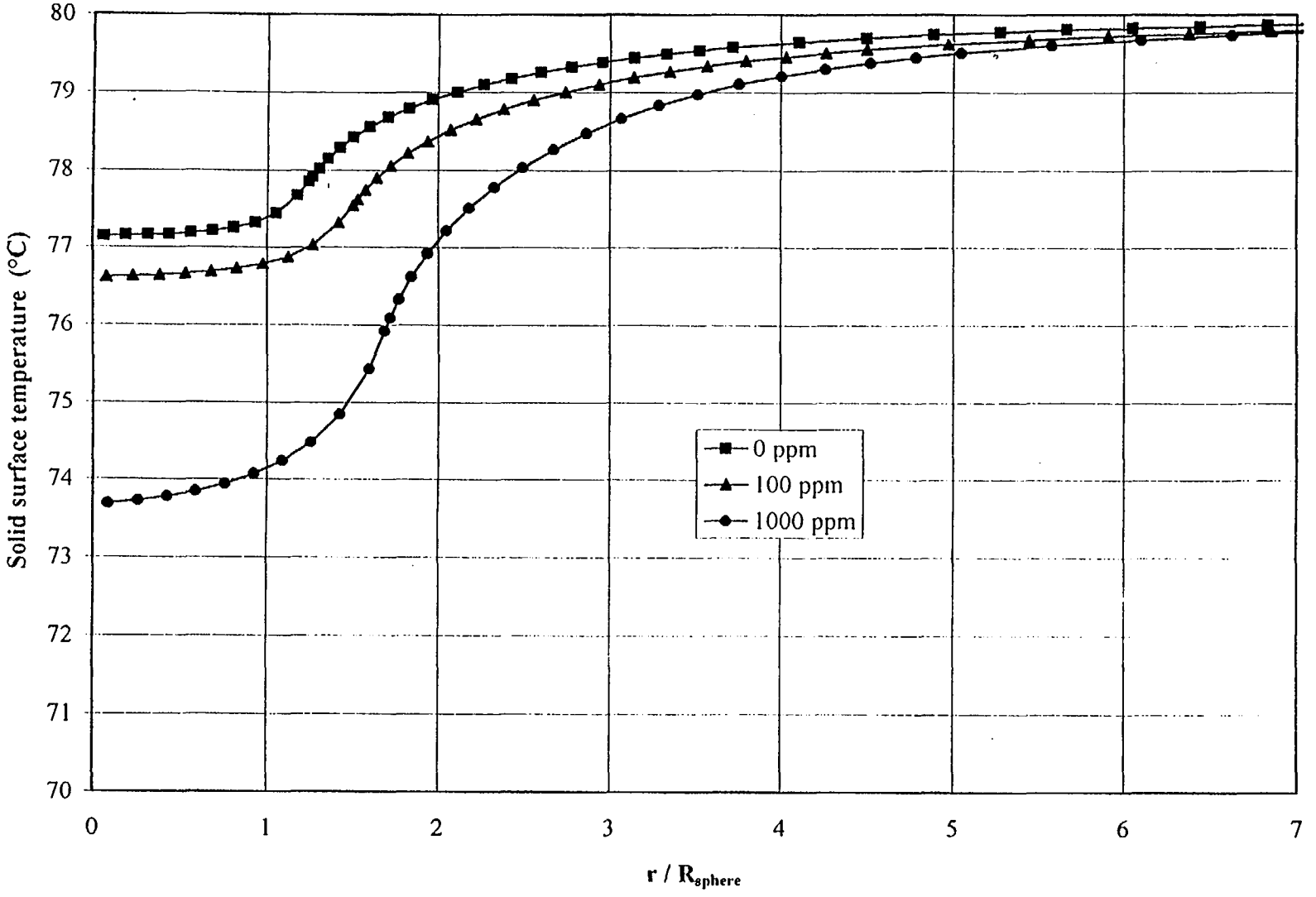
80
79
78
77
76
75
74
73
72
71
70
Solid surface temperature (°C)
0
1
2
3
4
5
6
7
r / R sphere
0 ppm
100 ppm
1000 ppm

Figure 9*b*

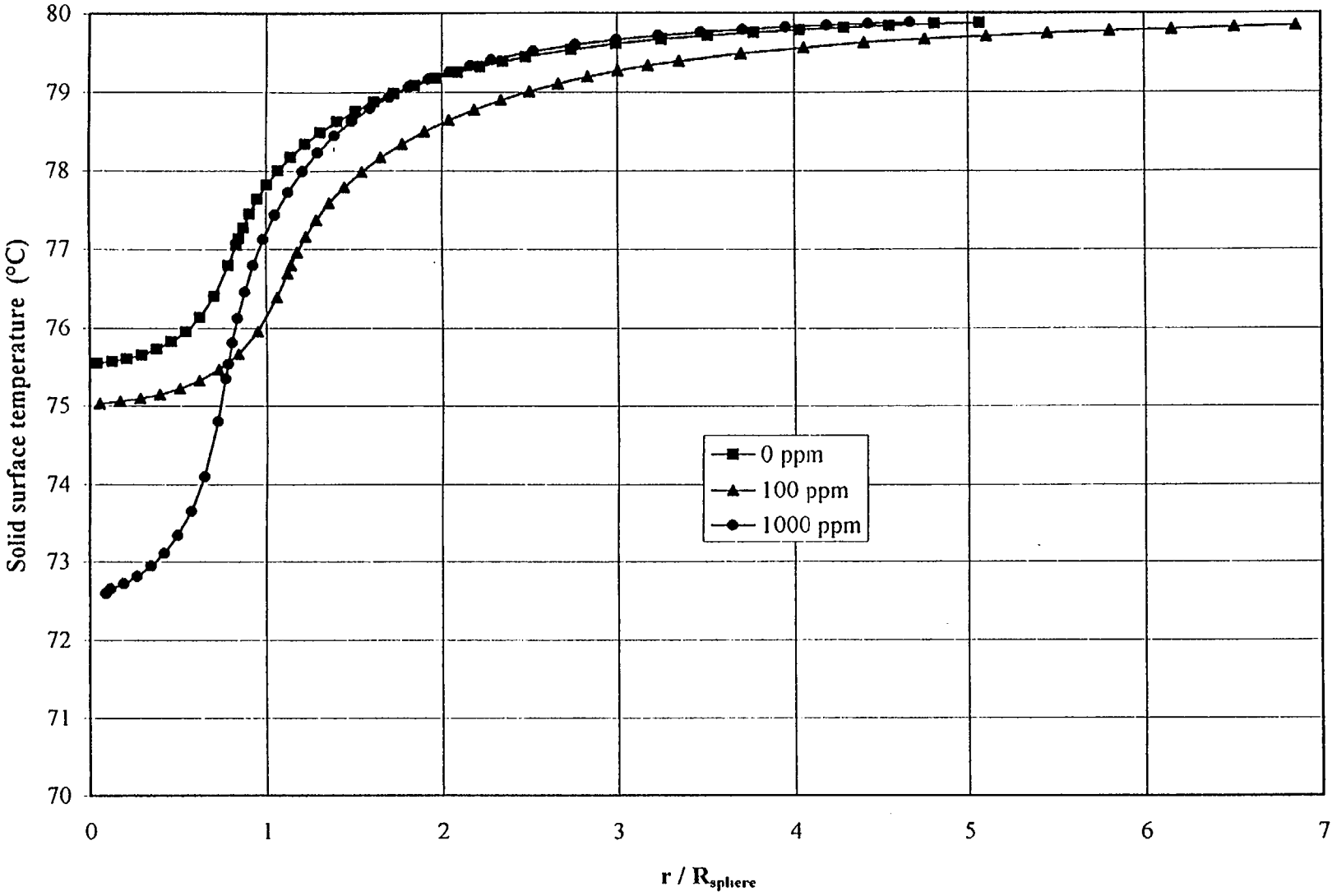
80
79
78
77
76
75
74
73
72
71
70
Solid surface temperature (°C)
0
1
2
3
4
5
6
7
r / R_spliere
0 ppm
100 ppm
1000 ppm

Figure 9c

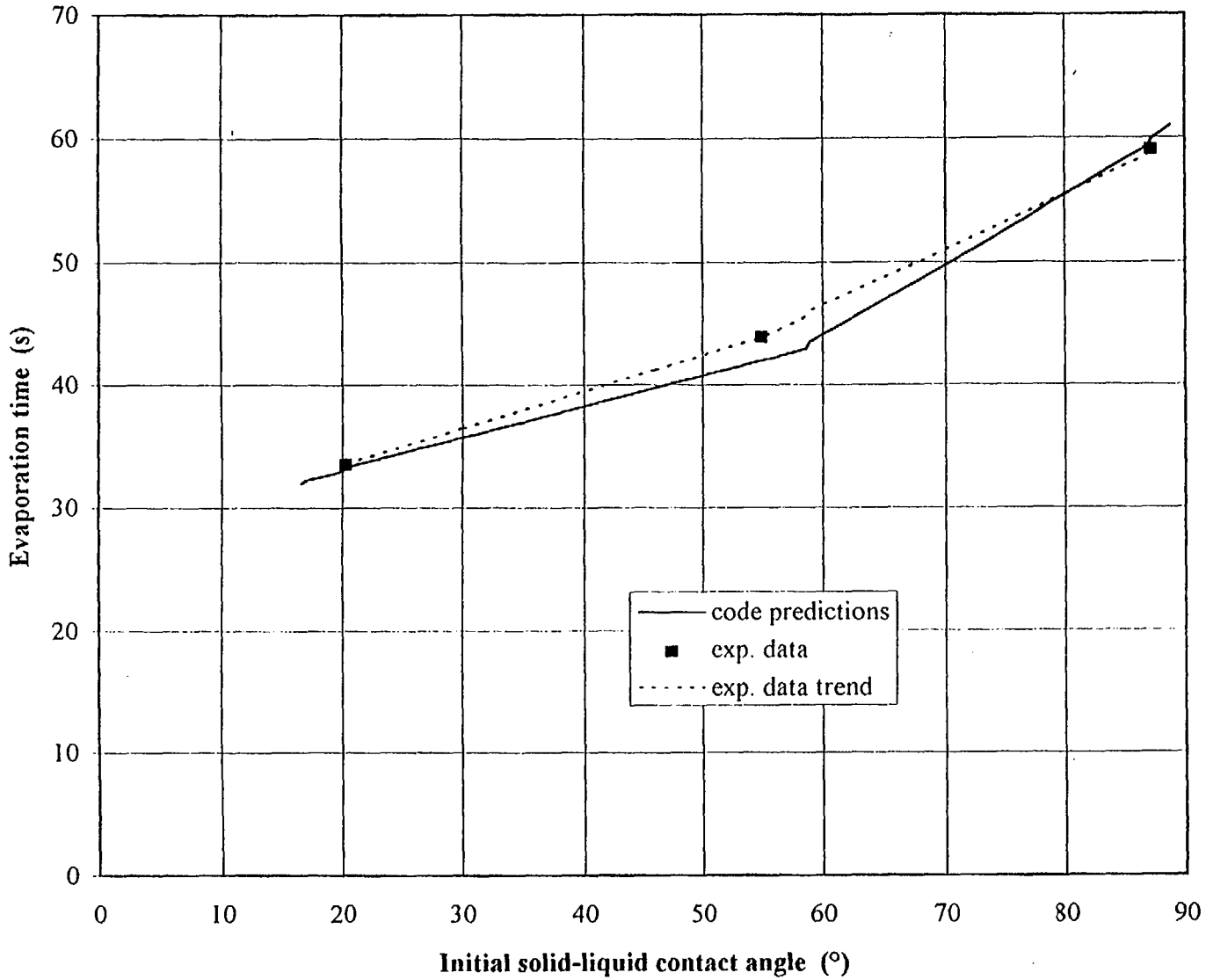

Figure 10 Effect of reducing contact angle on evaporation time of droplets on a stainless steel surface initially at 80°C.

APPENDIX B:

Effect of dissolved gasses in the water

S.C. Tinker & M. diMarzo, Effect of dissolved gasses on spray evaporative cooling with water (1995) unpublished manuscript.